Biomaterials 37 (2015) 289–298

Contents lists available at ScienceDirect

Biomaterials

journal homepage: www.elsevier.com/locate/biomaterials

[Pyr1]-Apelin-13 delivery via nano-liposomal encapsulation attenuates pressure overload-induced cardiac dysfunction

Vahid Serpooshan [a, b], Senthilkumar Sivanesan [c], Xiaoran Huang [c], Morteza Mahmoudi [a, c, d], Andrey V. Malkovskiy [c], Mingming Zhao [a], Mohammed Inayathullah [c], Dhananjay Wagh [c], Xuexiang J. Zhang [c], Scott Metzler [a], Daniel Bernstein [a, b], Joseph C. Wu [b], Pilar Ruiz-Lozano [a, b], Jayakumar Rajadas [b, c, *]

[a] Stanford University, Department of Pediatrics, 300 Pasteur Dr., Stanford, CA 94305, USA
[b] Stanford Cardiovascular Institute, Stanford University School of Medicine, Stanford, CA 94305, USA
[c] Biomaterials and Advanced Drug Delivery Laboratory, Stanford University School of Medicine, Stanford, CA 94305, USA
[d] Division of Cardiovascular Medicine, Department of Medicine, Stanford University School of Medicine, Stanford, CA 94305, USA

ARTICLE INFO

Article history:
Received 17 July 2014
Accepted 29 August 2014
Available online 13 October 2014

Keywords:
[Pyr1]-Apelin-13
Nanocarrier
TAC
Hypertrophy
Liposomal encapsulation
Sustained release

ABSTRACT

Nanoparticle-mediated sustained delivery of therapeutics is one of the highly effective and increasingly utilized applications of nanomedicine. Here, we report the development and application of a drug delivery system consisting of *polyethylene glycol (PEG)-conjugated* liposomal nanoparticles as an efficient *in vivo* delivery approach for [Pyr1]-apelin-13 polypeptide. Apelin is an adipokine that regulates a variety of biological functions including cardiac hypertrophy and hypertrophy-induced heart failure. The clinical use of apelin has been greatly impaired by its remarkably short half-life in circulation. Here, we investigate whether [Pyr1]-apelin-13 *encapsulation in liposome nanocarriers,* conjugated with *PEG polymer on their surface, can prolong* apelin *stability in the blood stream and potentiate apelin beneficial effects in cardiac function.* Atomic force microscopy and dynamic light scattering were used to assess the structure and size distribution of drug-laden nanoparticles. [Pyr1]-apelin-13 encapsulation in PEGylated liposomal nanocarriers resulted in sustained and extended drug release both *in vitro* and *in vivo*. Moreover, intraperitoneal injection of [Pyr1]-apelin-13 nanocarriers in a mouse model of pressure-overload induced heart failure demonstrated a sustainable long-term effect of [Pyr1]-apelin-13 in preventing cardiac dysfunction. We concluded that this engineered nanocarrier system can serve as a delivery platform for treating heart injuries through sustained bioavailability of cardioprotective therapeutics.

1. Introduction

Cardiac hypertrophy is an adaptive response of the heart cells to elevated levels of biomechanical stress imposed by a variety of extrinsic and intrinsic stimuli including pressure or volume overload, familial/genetic cardiomyopathies, or loss of contractile mass from preceding infarction [1–3]. If sustained, hypertrophy often becomes pathological, accompanied by significant risk of arrhythmia, progression to heart failure, and sudden death [1,4,5]. At the molecular level, pathological hypertrophy is associated with re-induction of the so-called fetal gene program in which the fetal isoforms of genes responsible for regulating cardiac contractility and calcium handling (e.g. *β-MHC*) are upregulated [1,2,6,7]. At the cellular level, the main characteristics of ventricular hypertrophic growth are enhanced protein synthesis and an increase in size of cardiomyocytes [1,2]. As pathologic hypertrophy progresses, these changes in molecular and cellular phenotypes are accompanied by an increase in apoptosis, fibrosis, chamber dilation, and decreased systolic function [1].

The murine model of transverse aortic constriction (TAC) is one of the most common experimental models used to study pressure overload-induced ventricular hypertrophy and elucidate the key signaling processes involved in the cardiac hypertrophic response and its progress to heart failure [8–11]. TAC initially results in compensated hypertrophy, frequently associated with a transient improvement in myocardial contractility; however, chronic hemodynamic overload leads to maladaptive hypertrophy

* Corresponding author. Biomaterials and Advanced Drug Delivery Laboratory, Stanford University School of Medicine, 1050 Arastradero Road, Room A148, Palo Alto, CA 94304, USA. Tel.: +1 650 724 6806; fax: +1 650 724 4694.
E-mail addresses: jayraja@stanford.edu, jrajadas@gmail.com (J. Rajadas).

http://dx.doi.org/10.1016/j.biomaterials.2014.08.045
0142-9612/

accompanied by ventricular dilatation and heart failure [8,10,12,13]. The TAC model has been utilized as a platform for examining the utility of pharmacological or molecular interventions that may limit hypertrophy or attenuate the hypertrophy-induced cardiac dysfunction [8,10].

Recent studies have shown that exogenous apelin plays a critical role in ameliorating cardiac dysfunction and/or remodeling in various animal models of cardiac disease such as myocardial infarction, ischemia reperfusion, and hypertrophy (e.g. Refs. [14–16]). Apelin is an endogenous peptide ligand for the G-protein-coupled AplnR (aka APJ), known to be involved in a broad range of physiological functions, including maintaining body fluid homeostasis, blood pressure, obesity, and heart development and function [17–20]. Although, AplnR and its recently identified ligand, apelin, show high levels of mRNA expression in the heart, their functional significance in the cardiovascular system is not yet fully understood [18,21]. Apelin is synthesized as a 77-amino acid peptide processed into various C-terminal fragments, including: apelin-36, apelin-19, apelin-17, apelin-13, and [Pyr1]-apelin-13 [22,23]. [Pyr1]-apelin-13 has been recognized as the predominant isoform of apelin in human plasma and cardiac tissue [22,24–26].

Extensive clinical use of [Pyr1]-apelin-13 has been seriously hampered due to the unstable nature of the peptide in both *in vitro* and *in vivo* conditions [43,44]. The plasma instability of apelin is due to the rapid degradation of the peptide [22,25,26,45] which results in significantly short plasma half-life (<8 min) [46]. Nanocarrier drug formulations have been found beneficial for the sustained delivery of therapeutic compounds in various cardiac disease [27–29]. Among a variety of nanocarriers, liposomes are widely considered as suitable vesicles for potential targeted drug delivery [30–32]. In particular, liposomal peptide delivery platform caters to various biological needs [33–35]. To promote effective drug targeting, ligands for specific cell surface receptors need to be incorporated in the nanocarriers [36]. Liposomes encapsulating drugs can perform this function via utilizing a variety of loading methods [37–39]. Considering the fact that surface modifications of liposomes can help to improve the drug release properties of these carriers, a considerable amount of research has been focused on the liposome-drug interactions [40–42].

In this study, a novel liposomal nanocarrier system, incorporated with *polyethylene glycol (*PEG) polymer on the surface, was utilized in order to deliver [Pyr1]-apelin-13 as a therapeutic molecule into the injury site in a TAC mouse model. The effect of sustained release of [Pyr1]-apelin-13 on the hypertrophic response of the heart was assessed.

2. Materials and methods

2.1. Liposome preparation and [Pyr1]-apelin-13 encapsulation

Lipids used in the preparation of liposomes include 1,2-distearoyl-sn-glycero-3-phosphoethanolamine-N-[amino (polyethylene glycol)-3400] (DSPE-PEG(3400)-NH2) (Laysan Bio, Inc.), cholesterol (Sigma), and 1,2-distearoyl-sn-glycero-3-phosphocholine (DSPC) (Avanti polar lipids, Inc.). PEG-containing liposome (lipoPEG) was prepared by dissolving cholesterol (5 mg), NH2-PEG-DSPE (2 mg), and DSPC (10 mg) in 1 mL of chloroform in a round-bottom (RB) flask. The mixture was evaporated in a rotary evaporator under vacuum to make a thin layer of molecules in the RB flask. The lipid layer was hydrated by the addition of 1 mL double distilled water sonicated for 30 min to obtain a turbid liposome solution. The solution was frozen and lyophilized to obtain solvent-free dry liposomes. [Pyr1]-apelin-13 was encapsulated by hydrating the liposomes (17 mg) with 3.3 mg of pyroglutamyl [Pyr1]-apelin-13 in 1 mL double distilled water followed by 30 min sonication. In order to get the maximum encapsulation, the mixture was frozen and lyophilized again followed by rehydrating it with 1 mL double distilled water and sonicated before use. Hereby, liposome-PEG-[Pyr1]-apelin-13 (lipoPEG-PA13) was prepared.

2.2. Atomic force microscopy

Samples were prepared for atomic force microscopy (AFM) by drop-casting and drying under vacuum of 10 μL droplets with a liposome concentration of 0.01 mg/mL on the surface of clean silicon wafers. AFM imaging was performed with Park Systems NX10 (Suwon, Korea) AFM instrument. Samples were imaged in semi-contact mode with standard commercial cantilevers ($k = 5–9$ N/m, $R < 10$ nm), at 1 Hz scan speed and ~30% oscillation damping.

2.3. Dynamic light scattering measurements

Solutions were prepared from dry lyophilized liposomes at a concentration of 1 mg/mL. Samples were vortexed until no visible sediment could be detected. Dynamic Light Scattering (DLS) measurements were performed using Brookhaven 90 plus DLS nanosizer (Brookhaven Instruments Corporation, Holtsville, NY). The autocorrelation function was approximated manually with a single-relaxation process using second-order term for the cumulant analysis of particle polydispersity.

2.4. In vitro [Pyr1]-apelin-13 release study

In vitro release of [Pyr1]-apelin-13 was measured using rapid equilibrium dialysis (RED) plate assay (Thermo Scientific Co.). The plate is composed of disposable high-density polypropylene and equilibrium dialysis membrane inserts compartmentalized in to buffer and sample chambers. Each insert is comprised of two side-by-side chambers separated by an O-ring-sealed vertical cylinder of dialysis membrane with molecular weight cutoffs (12 kDa). Stock solution of liposome-PEG-[Pyr1]-apelin-13 (lipoPEG-PA13) was prepared in 2 mL PBS containing 100 nM concentration of [Pyr1]-apelin-13 peptide. The lipoPEG-PA13 sample (750 μL) and the buffer PBS (500 μL) were placed into the corresponding sample (donor) and buffer chambers, respectively. The entire unit was then covered with sealing tape and incubated at 37 °C on an orbital shaker at approximately 300 rpm. At each time point of analysis, a volume of 10 μL was withdrawn from the buffer side of the chamber and replaced with the same volume in return. At 0 h (start point) and 24 h (end point), a volume of 10 μL was collected from both the sample (donor) and the buffer chambers. Despite the long duration of incubation time (24 h), there was no increase in the sample volume due to the hydrostatic pressure. All drug release experiments were done with samples in triplicates. The vials containing collected sample (donor) and buffer solutions were stored at 4 °C before mass spec analysis.

2.5. Liquid chromatography/mass spectrometry analysis

The concentration of [Pyr1]-apelin-13 released from liposome was measured using liquid chromatography (LC, Shimadzu-LC-20AB Prominence Liquid Chromatogram) coupled with a mass spectrometry (MS) device (4000 Q Trap). Briefly, the collected 10 μL volume of either buffer or donor was added to 20 μL water and 30 μL methanol to precipitate the peptide. Chromatographic separation was performed on a C18 reversed-phase column (XBridge C18, 3.0 × 150 mm, 3.5 μm particle size) by injecting 10 μL per sample. Gradient elution was employed at a flow rate of 0.3 mL/min with the following solvent and conditions: 0–0.5 min 20% acetonitrile/0.1% formic acid, water/0.1% formic acid/5 mM ammonium acetate, 0.5–7 min gradient from 20% to 90%; 7–8 min 90%; 8–12 min 20%. Based on our established protocol, mass spectrometric detection was conducted specifically at the Q1 (512.060 mass in Da) and Q3 (263.000 mass in Da) regions accomplished with an electrospray ionization (ESI) source in positive ion mode at 5.5 kV spray voltage. Data acquisition was carried out by the AB Sciex Analyst version 1.6.1 software. The concentration of [Pyr1]-apelin-13 in the sample chamber and those released in to the buffer chamber were measured from the calculated peak areas relative to the internal standard.

2.6. In vitro assessment of [Pyr1]-apelin-13 effect on APJ translocation

The influence of [Pyr1]-apelin-13 formulation (lipoPEG-PA13) – versus commercially available [Pyr1]-apelin-13 peptide – on the APJ translocation efficacy was tested *in vitro*, using human embryonic kidney (HEK) 293 cells overexpressing GFP-APJ as described elsewhere [47]. HEK cells, transfected with human APJ, were cultured in DMEM containing 1% penicillin/streptomycin and 10% FBS. Following 60 min incubation with lipoPEG-PA13, the GFP-APJ fluorescence was tracked using a high-resolution confocal laser scanning microscope (Zeiss LSM510 Meta).

2.7. Mouse model of TAC – [Pyr1]-apelin-13 nanocarriers administration

All procedures involving animal use, housing, and surgeries were approved by the Stanford Institutional Animal Care and Use Committee (IACUC). Animal care and interventions were provided in accordance with the Laboratory Animal Welfare Act. Male 10–13 weeks old C57BL/6J mice were purchased from Jackson Laboratories (Bar Harbor, ME, USA) and divided randomly into five groups: I and II) sham controls with no aortic constriction, treated with either saline or [Pyr1]-apelin-13 formulation, III to V) mice with TAC injury treated with either saline, regular [Pyr1]-apelin-13, or lipoPEG-PA13 ($n > 4$, Fig. 1A–D).

For constriction of transverse thoracic aorta [8], mice were anesthetized using an isoflurane inhalational chamber, followed by endotracheal intubation using a 22-gauge angiocatheter (Becton, Dickinson Inc., Sandy, Utah) connected to a small animal ventilator (Harvard Apparatus, Holliston, MA). A left thoracotomy was performed via the fourth intercostal space, the transverse aorta was identified, and a 6.0 silk suture was placed between the innominate and left carotid arteries. The suture

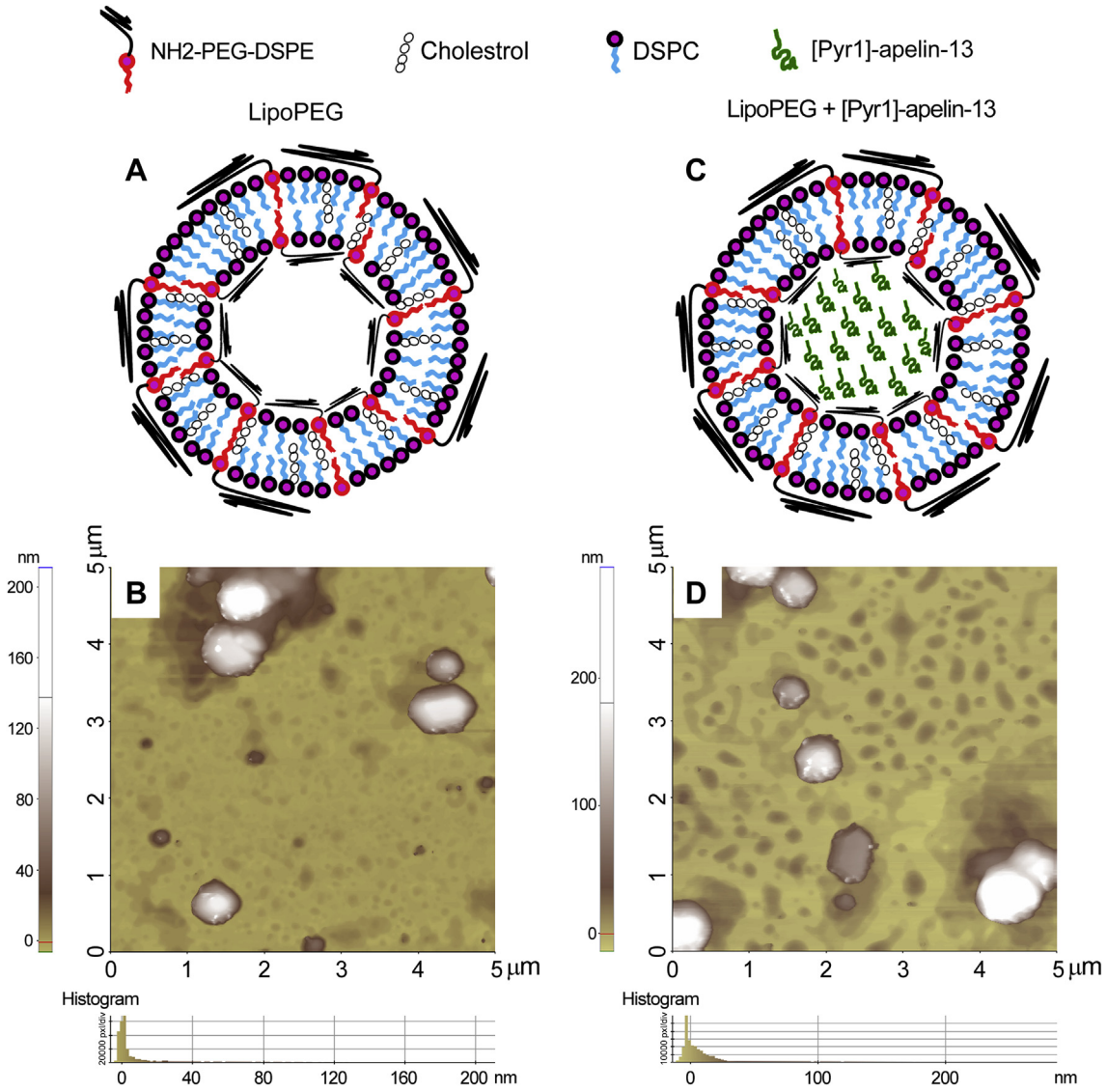

Fig. 1. Schematic representation (top) and AFM images (bottom) demonstrating the structure of empty PEG liposomes (A and B, respectively), and PEG liposomes encapsulated with [Pyr1]-apelin-13 (C and D, respectively). Panels B and D demonstrate the morphology of the nanocarrier systems used in this study.

was tightened around a $27^{1/2}$ gauge blunt needle, placed parallel to the aorta (Fig. 1B) to induce a constriction of ~0.4 mm in diameter. In sham control mice, an identical procedure was conducted, except for the constriction of the aorta. Mice received [Pyr1]-apelin-13 or saline (control) intraperitoneally (300 µg/kg body weight) at days 1 and 7 post-surgery.

2.8. Echocardiography

In vivo heart function was evaluated by echocardiography at 1 day prior to surgery (baseline) and on days 1, 7, and 14 post-surgery (Fig. 1A). Two-dimensional (2D) analysis was performed using a GE Vivid 7 ultrasound platform (GE Health Care, Milwaukee, WI) equipped with a 13 MHz transducer. Mice were anesthetized with isoflurane (2% inhalation). 2D clips and M-mode images were obtained in the short axis view from the mid-LV at the tips of the papillary muscles. Fractional shortening (FS), LV internal diameter at end diastole (LVIDd) and systole (LVIDs), and posterior LV wall thickness at end diastole (LVPWd) were measured. A minimum number (n) of 4 mice per study group was used for the echo evaluations. Measurements were performed by two independent observers blinded to study groups.

2.9. Measurement of [Pyr1]-apelin-13 concentration in blood plasma

24 h post-surgery, sham and TAC operated mice were injected intraperitoneally with either saline or the [Pyr1]-apelin-13 nanocarriers (lipoPEG-PA13) at 0.4 mg/kg body weight. Wild type mice without surgery and with no injections were used as controls to measure the apelin-13 baseline levels. At days 1, 4, and 6 post injection, mice were anesthetized with isoflurane (100 mg/kg, inhalation) and blood was collected using two different techniques: 1) from the Orbital Sinus (Retro-orbital technique) by inserting the tip of a microhematocrit blood tube into the corner of the eye socket, underneath the eyeball, and directing the tip at towards the middle of the eye socket at a 45-degree angle (details in Ref. [48]). 2) from the tail vein; using a straight edge razor, approximately 1 cm of the tail was quickly removed. For additional samples at later time point, blood sample was obtained by removing ~2–3 mm of additional tail (details in Ref. [48]). The blood obtained from either approaches was placed in a polypropylene tube containing 0.1 volume of 3.8% sodium citrate, pH 7.4. Plasma was then prepared by centrifuging the samples at 15,000 *g* for 10 min (at 4 °C) using a table-top microcentrifuge (Eppendorf 5424R). Aliquots were stored at −80 °C before analysis.[Pyr1]-apelin-13 concentrations were determined by commercial enzyme linked immunosorbent assay (ELISA) kits according to the manufacturers' instructions (Apelin EIA kit, Phoenix Pharmaceuticals, Burlingame, CA). Each assay was performed in duplicates. Standard curve was fitted using the 4-parameter logistic (4 PL) nonlinear regression model [47].

2.10. Histological analysis

Histological analysis was performed following standard protocols for paraffin embedding. Mounted heart samples were stained for Masson's trichrome (TC, to label muscle fibers in red, collagen in blue, cytoplasm in pink, and nuclei in dark brown). A minimum of 4 sections per sample were used.

2.11. Statistical analysis

The number of samples (n) used in each experiment is noted in the text. Dependent variables are expressed as means ± SEM, unless noted otherwise. The

differences in the means were tested using ANOVA and Student *T*-test to check for statistical significance ($P < 0.05$).

3. Results

3.1. AFM characterization of liposomes and liposome encapsulating [Pyr1]-apelin-13

AFM imaging of the particles, performed in tapping mode, generated the topography maps of the PEG liposomes (Fig. 1). Both the empty liposomes and PEG liposomes encapsulating [Pyr1]-apelin-13 (Fig. 1A and C, respectively) exhibited semi-spherical structure with relatively narrow size distribution. The lipoPEG-PA13 nanoparticles formed objects akin to "sunny side up" fried eggs. There was only a slight difference in the morphology and height of the particles in empty *versus* apelin-13-loaded conditions (Fig. 1B and D, respectively).

3.2. Particle size characterization using dynamic light scattering

Dynamic light scattering (DLS) was used to analyze the size distribution of the empty lipoPEG particles and the particles laden with [Pyr1]-apelin-13, in the absence or presence of 0.5% BSA (Fig. 2A). The average size of the lipoPEG alone was estimated to be 0.57 ± 0.02 (SD) μm. Upon inclusion of 0.5% BSA, there was almost no change in size (0.53 ± 0.02 (SD) μm) for lipoPEG particles. However, [Pyr1]-apelin-13 encapsulation in lipoPEG showed a striking reduction in particle size to 0.06 ± 0.00 μm. Inclusion of 0.5% BSA to particles with encapsulated [Pyr1]-apelin-13 increased their size to 0.22 ± 0.02 (SD) μm.

3.3. Liposomal encapsulation promotes sustained in vitro release of [Pyr1]-apelin-13

[Pyr1]-apelin-13 encapsulation in lipoPEG particles (lipoPEG-PA13) resulted in sustained and extended drug release under physiological conditions *in vitro* when monitored over a 24 h period at different time intervals (Fig. 2B and C). The peak [Pyr1]-apelin-13 release profile was obtained between 15 and 20 h period followed by a saturation curve at the end of 24 h. [Pyr1]-apelin-13 release from lipoPEG-PA13 was accelerated (18.6 μg/mL) in the presence of 0.5% BSA (Fig. 2C).

3.4. LipoPEG-PA13 nanocarriers promote APJ translocation in vitro

The *in vitro* effect of [Pyr1]-apelin-13 nanocarriers on APJ translocation was analyzed in APJ-GFP^{+} HEK293 cells and compared to that induced by commercially available [Pyr1]-apelin-13 (300 nM in culture media [47], Fig. 3). Tracing the fluorescent APJ receptors using high-resolution confocal microscopy demonstrated that lipoPEG-PA13 nanocarriers stimulated APJ translocation from the cell membrane towards the cytoplasm more efficiently than that caused by the regular [Pyr1]-apelin-13. The lipoPEG-PA13 nanocarriers also exhibited a qualitatively higher GFP signal after 60 min (Fig. 3).

3.5. Treatment with lipoPEG-PA13 nanocarriers attenuates TAC-induced cardiac dysfunction in vivo

The lipoPEG-PA13 was administered *in vivo* in TAC operated mice and sham-operated controls by means of single weekly injections for two weeks (Fig. 4). Serial echocardiography at baseline and days 1, 8, and 15 after injury demonstrated significant beneficial effects of lipoPEG-PA13 administration in inhibiting pressure overload-induced LV dysfunction (Fig. 5). No significant differences

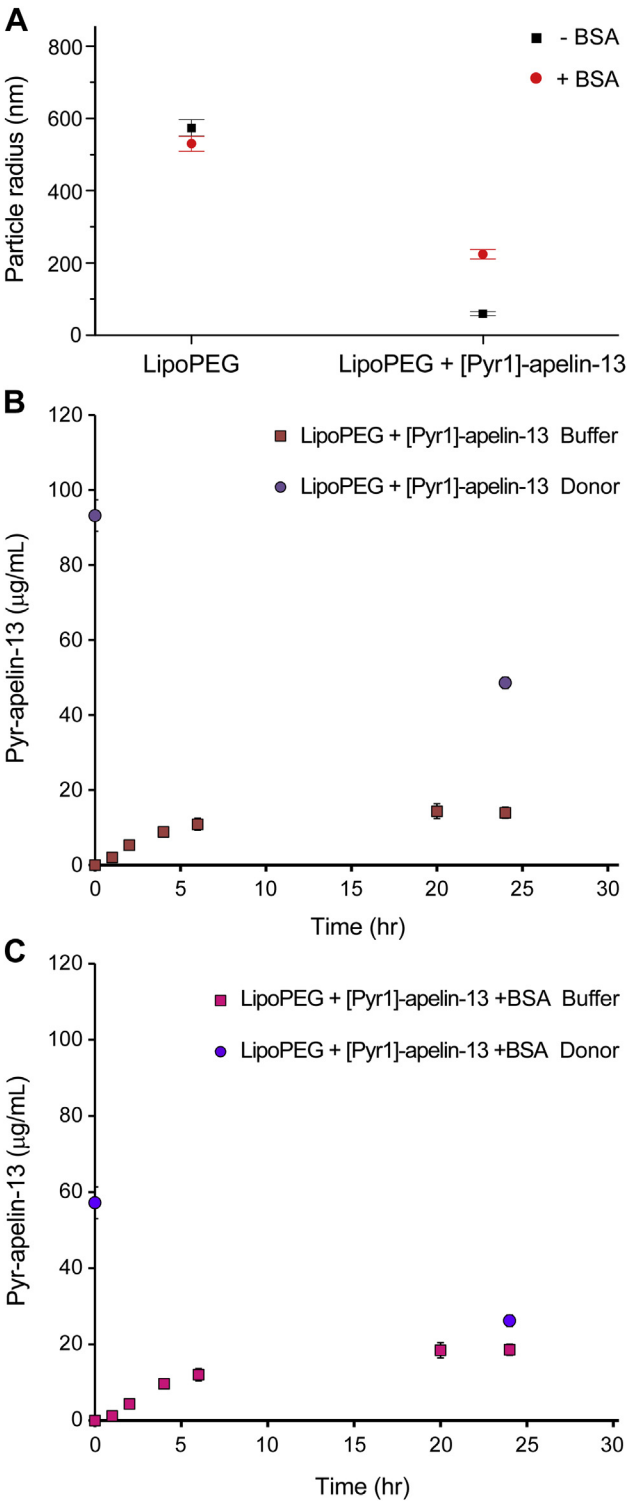

Fig. 2. A: DLS data demonstrating the liposome particle sizes. Error bars indicate standard deviations of liposome sizes based on cumulant analysis. B and C: time course analysis of [Pyr1]-apelin-13 release from liposomes in the absence (B) and presence (C) of %0.5 BSA, by rapid equilibrium dialysis plate assay. The quantity (μg/mL) of [Pyr1]-apelin-13 released from donor to buffer reservoir over a 24 h time course at various intervals is indicated.

were observed in echo parameters of the three TAC groups at day 1 post-surgery (Fig. 5A). In saline-treated animals (TAC + saline), TAC resulted in LV hypertrophic growth, chamber dilation, and a significant drop in cardiac function at days 8 and 15 post operation

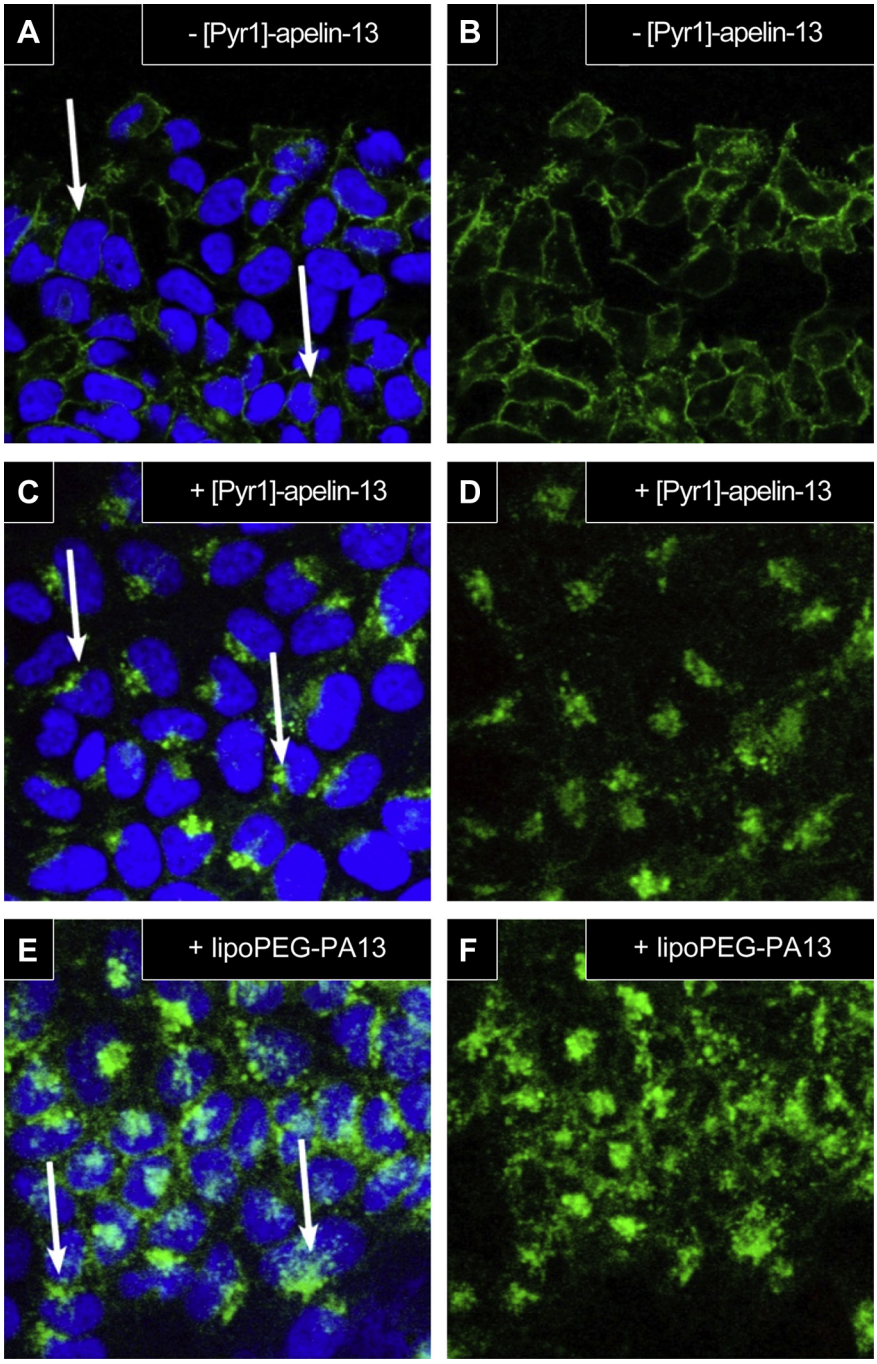

Fig. 3. *In vitro* assessment of the effect of the [Pyr1]-apelin-13 nanocarriers on the APJ (green) translocation (white arrows) in HEK APJ-GFP + cells ($t = 60$ min). (A) and (B): negative controls, without [Pyr1]-apelin-13. (C) and (D): regular [Pyr1]-apelin-13 effect. (E) and (F): the effect of addition of lipoPEG-[Pyr1]-apelin-13 nanocarriers. DAPI staining the nuclei (blue). (For interpretation of the references to color in this figure legend, the reader is referred to the web version of this article.)

(Fig. 5B and C, respectively). In contrast, the application of [Pyr1]-apelin-13 nanocarriers (TAC + lipoPEG-PA13) blunted LV dilation at both end-diastole and systole (LVIDd and LVIDs, respectively), attenuated the increase in posterior wall thickness (LVPWd) at day 15, and preserved cardiac contractility (FS) (Fig. 5B–D). In contrast, the administration of commercially available [Pyr1]-apelin-13 (TAC + [Pyr1]-apelin-13) had a more modest effect in diminishing the hypertrophic response to pressure overload. Sham operated groups injected with either saline (data now shown for the simplicity of the graphs) or lipoPEG-PA13 showed no significant changes in cardiac dimensions or function. Thus, lipoPEG-PA13 attenuated pressure overload-induced cardiac dysfunction up to two weeks post injury.

In order to further assess the effect of [Pyr1]-apelin-13 nanocarriers on heart tissue structure and remodeling, mice were sacrificed two weeks post injury and hearts were analyzed. Histology (trichrome staining) of heart sections demonstrated no significant changes in cardiac morphology of sham controls, either in saline or [Pyr1]-apelin-13 treated animals (Fig. 5E). TAC + saline-treated mice showed a remarkable increase in the size of LV and the amount of fibrotic tissue. TAC mice treated with lipoPEG-PA13 showed reductions in both the size of the LV and the extent of

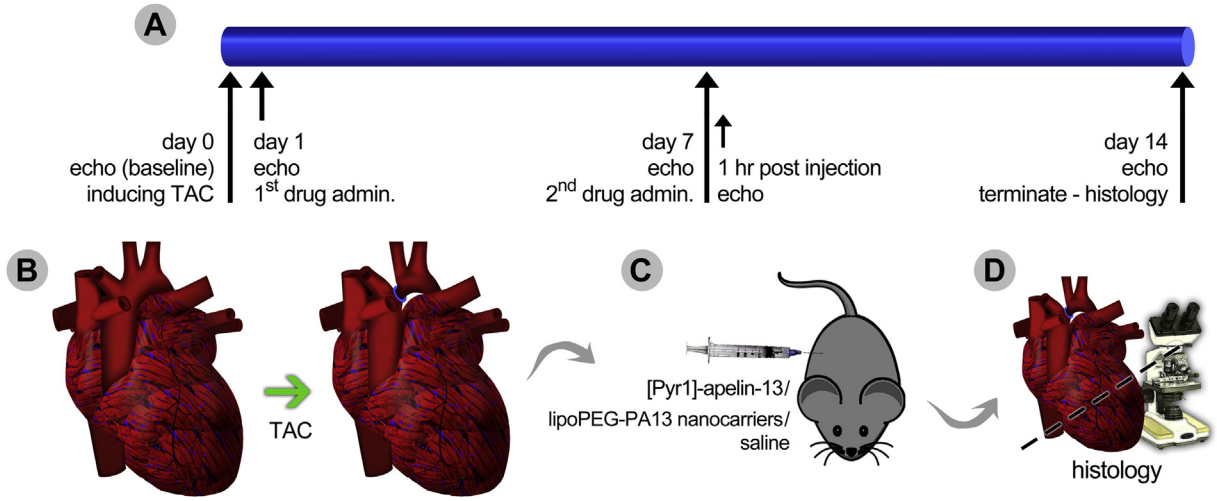

Fig. 4. Schematic representation of the experimental procedure used to assess the effect of lipoPEG-[Pyr1]-apelin-13 nanocarriers administration *in vivo*, on the TAC-induced cardiac hypertrophy in mouse.

cardiac fibrosis, when compared to TAC + saline and TAC mice treated with regular [Pyr1]-apelin-13 (Fig. 5E).

3.6. Liposomal encapsulation promotes sustained release of [Pyr1]-apelin-13 in vivo

IP administration of lipoPEG-PA13 in both sham-operated and TAC mice resulted in significantly elevated levels of [Pyr1]-apelin-13 in blood plasma at days 1, 4, and 6 post injection, when compared to those in control animals (injected with saline, or not injected, WT) (Fig. 6A and B). The peak [Pyr1]-apelin-13 levels in blood plasma in the TAC and sham mice were obtained at days 1 and 4 post injection, respectively. Moreover, in comparison between sham (■) and TAC (■) mice injected with lipoPEG-PA13, [Pyr1]-apelin-13 concentration in TAC mice was significantly greater than that in sham group at each time point (except day 4).

4. Discussion

Recent studies have shown that the loss of apelin function, together with deficiency of its receptor APJ, correlated with cardiovascular disease [20,49,50]. Some studies have consistently suggested that decreased plasma or myocardial levels of apelin/APJ levels can lead to the incidence of various cardiac defects [14,51,52]. To date, a significant amount of research has evaluated the role of apelin administration in regulating cardiac dysfunction in various models of heart disease, introducing this peptide as an attractive target for pharmacotherapy studies in the setting of heart failure [18,21,50,44]. Among other beneficial effects, apelin delivery using osmotic pumps has been shown to prevent aortic aneurism [53], ameliorate myocardial reperfusion injury [54], induce vasodilatation [46], and prevent deleterious hypertrophy remodeling [47]. However, the success of conventional systemic drug administration approaches is limited due to several factors including the lack of targeting capability into a pathological site, poor control of sustained drug delivery during the desired therapeutic time, the necessity of a high dose at the target site, nonspecific toxicity, and peptide instability [55–57]. Here, we investigated the use of a liposome nanocarrier system for sustained delivery of exogenous [Pyr1]-apelin-13 and its effect on TAC-induced cardiac hypertrophy in the mouse model.

In order to increase the stability of the nano-liposome in the circulation, the absorbance of the opsonin-based proteins at the surface of nanoparticles should be prevented [58]. One of the well-recognized approaches for enhancing stability of nano-size materials in circulation is to coat their surfaces by polyethylene glycol (PEG) polymers [59]. PEG polymer has been used extensively for the covalent alteration of biological macromolecules and surfaces for various biomedical and pharmaceutical applications [60,61]. This polymeric shell can prevent plasma's opsonin proteins interactions with the surface of nanocarriers and hence rescue their removal by reticuloendothelial system [30,62–64]. PEGylation process increases the molecular mass of protein complexes and shields them against proteolytic enzymes, hence, prolongs their circulation half-life [60,65]. Thereupon, a lower number of injections or a less chronic drug administration will be required to maintain plasma concentrations of the PEGylated proteins or peptides [66]. In this study, PEG polymer was incorporated onto the surface of the liposome carriers in order to improve blood plasma stability during *in vitro* and *in vivo* experiments.

AFM imaging of the nanocarriers demonstrated the integration of [Pyr1]-apelin-13 into the liposomal particles, with the formation of a mostly homogeneous structure without a clearly defined core and shell (Fig. 1). If we approximate the shape of the two particles in Fig. 1A with a half of an oblate ellipsoid, the volume would be:

$$V_{\frac{1}{2}\ \text{oblate ellipsoid}} = \frac{1}{2}\cdot\frac{4}{3}\pi a^2 b \qquad (1)$$

where a and b are halves of long and short axes of the ellipsoid, respectively. The same particles would take a shape of a sphere in solution, the diameter of which would be:

$$D = 2\cdot\left(\frac{V}{4/3\,\pi}\right)^{1/3} \qquad (2)$$

The diameters, obtained in such a fashion are about 0.5 μm, which is in close agreement with the DLS data (Fig. 2A). Using this approximation, the typical volume and, therefore, the solution size of BSA-coated liposomes were calculated to be about the same.

The DLS characterization of plain liposomes (lipoPEG) and those encapsulated with [Pyr1]-apelin-13 demonstrated relatively high monodispersity of all sets of particles which was not significantly affected by the addition of BSA (Fig. 2A). Interestingly, it appears that the addition of BSA drives the particle size to 0.5 μm, which can be related to the general stability of a BSA-coated particle in a water

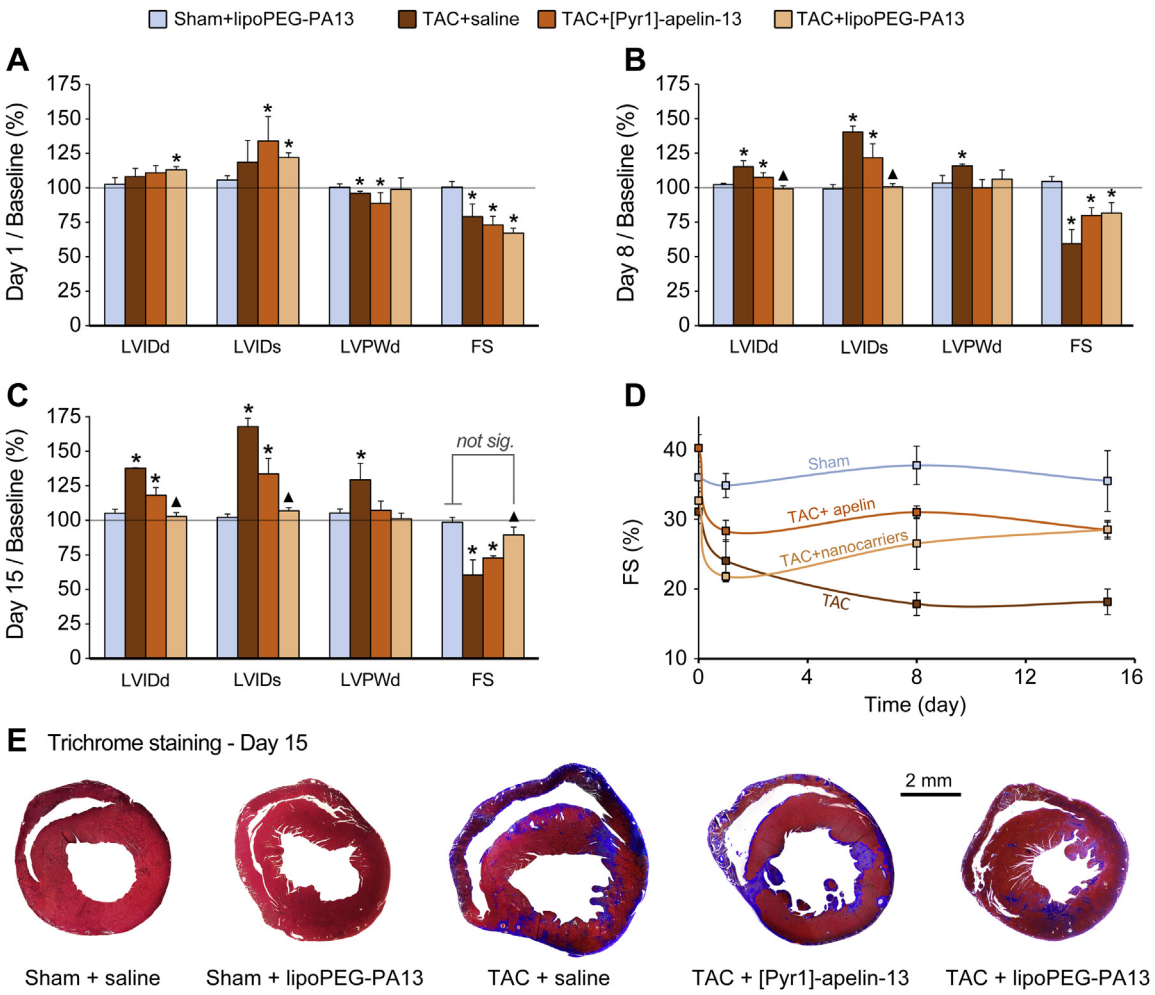

Fig. 5. Percentage changes in echocardiographic parameters compared to baseline (divided to the pre-surgery values), at days 1 (A), 8 (B), and 15 (C) post-surgery (TAC). Moreover, panel (D) demonstrates the absolute fractional shortening (FS) values for the four different groups as a function of time post-surgery. Saline (sham controls), [Pyr1]-apelin-13, or lipoPEG-[Pyr1]-apelin-13 (lipoPEG-PA13) were injected IP (300 μg/Kg body weight) at days 1 and 7 post-surgery. While sham controls, either injected with saline (not shown) or lipoPEG-PA13 nanocarriers ■, showed no significant changes in the heart function over 2-week time period, TAC hearts with saline treatment ■ showed significant decline in cardiac contractility (fractional shortening, FS) and an increase in LV diameter (LVID) as well as LV posterior wall thickness (LVPW), indicating a hypertrophic response and cardiac dysfunction. Administration of commercial [Pyr1]-apelin-13 ■ resulted in slight inhibition of cardiac remodeling and increase in FS, when compared with TAC controls. The greater effect however, was observed in the group treated with lipoPEG-PA13 carriers ■ in which cardiac contractility (FS) was significantly improved compared with those in other TAC groups (D), and hypertrophic remodeling was significantly inhibited. As shown in panel (D), the four animal groups of this study showed varying levels of FS at the baseline. Considering these differences, the significant effect of nanocarriers treatment in improving FS is evident. A minimum of four replicates were analyzed for each group. Statistical analysis was performed using one-way ANOVA test. Values are reported as average ± SEM. *: $P < 0.05$ compared to sham controls (■). ▲ : $P < 0.05$ compared to TAC injected with [Pyr1]-apelin-13 (■). E: Representative heart sections with Masson's trichrome staining for all experimental groups. While TAC caused a remarkable left ventricular hypertrophic growth along with a significant amount of fibrotic tissue in untreated TAC hearts, administration of [Pyr1]-apelin-13 or lipoPEG-PA13 nanocarriers resulted in remarkable inhibition of the LV growth, attenuating TAC-induced cardiac dysfunction, and diminishing fibrosis. Scale bar is 2 mm.

solution. The relatively large size of particles contributes to the extension of the release period, since it takes longer for the particles to get incorporated through the outer skin layers.

Considering the fact that sustained drug release is an important pharmacokinetic entity, the effect of lipoPEG (14 μg/mL) particles in sustained and prolonged *in vitro* release of [Pyr1]-apelin-13 over a 24 h time course was quite significant (Fig. 2B and C). [Pyr1]-apelin-13 release from lipoPEG-PA13 carriers was accelerated (18.6 μg/mL) in the presence of 0.5% BSA (Fig. 2C) suggesting that BSA had no effect in promoting the drug sustainability. Several studies have reported efficient targeting of protein or peptide based drugs via PEG liposome encapsulation [67–69]. Of particular note, PEGylated DSPE liposomes have shown great potential in promoting the sustained release of several peptide based drugs *in vitro* [70–72].

Enhanced *in vitro* efficacy of [Pyr1]-apelin-13 via nanoencapsulation was also demonstrated by no adverse effect on cell viability, and significantly increased APJ translocation in the HEK cells when compared to that induced by [Pyr1]-apelin-13 alone (Fig. 3, Suppl. Figs. 1 and 2). The cationic PEGylated Liposomes are recognized for their intricate ability to become incorporated into pre-formed vesicles, hence, improving cellular binding *in vitro* [73]. Cellular uptake of peptide-encapsulating PEGylated liposomes has been reported to take place through clathrin-mediated endocytosis pathway [74]. In our future study, we aim to elucidate the precise cellular binding and uptake mechanisms that are involved in these nanocarriers–cell interactions.

Administration of lipoPEG-PA13 nanocarriers after TAC demonstrated a significant benefit of the drug in attenuating pressure overload-induced cardiac dysfunction (Fig. 5). On day 8, the administration of lipoPEG nanocarriers resulted in significantly reduced LV dimensions ($P < 0.05$) when compared with those in regular [Pyr1]-apelin-13-treated mice, while there was no

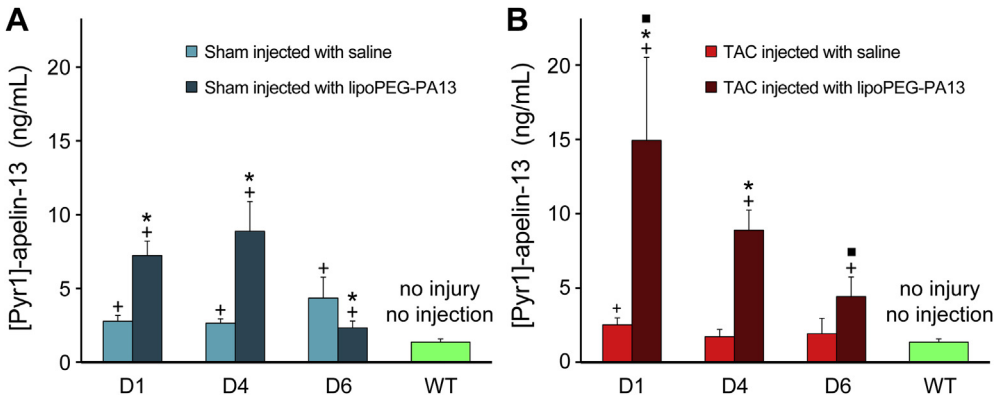

Fig. 6. [Pyr1]-apelin-13 release *in vivo*; using ELISA, the [Pyr1]-apelin-13 concentration in blood plasma was measured at 1, 4, and 6 days post IP injection, in A: Sham mice injected with saline (control ■) or lipoPEG-[Pyr1]-apelin-13 (lipoPEG-PA13) (■), and B: TAC mice injected with saline (control ■) or lipoPEG-PA13 nanocarriers (■). These were compared with [Pyr1]-apelin-13 concentration in blood plasma of wild type (WT) mice with no injury and no injections (■ A and B). In both sham and TAC animals, using the nanocarriers resulted in significantly elevated levels of [Pyr1]-apelin-13 in blood plasma up to 6 days post injection, compared to those in saline-injected animals as well as those in control WT mice. A minimum of four replicates were analyzed for each group. Statistical analysis was performed using one-way ANOVA test. Values are reported as average ± SEM. +: $P < 0.05$ compared to WT controls. *: $P < 0.05$ compared to same time, injected with saline. ■: $P < 0.05$ compared to sham at the same time, injected with lipoPEG-PA13 carriers.

significant difference in LV contractility (FS) (Fig. 5B). This suggests that at earlier time points, lipoPEG-PA13 administration effectively interfered with cardiac hypertrophic remodeling. At week 2, in contrast to the TAC mice treated with saline or regular [Pyr1]-apelin-13 (without carriers), administration of the lipoPEG-PA13 resulted in a significant improvement in LV contractility (FS) ($P < 0.05$). We have previously demonstrated that naked [Pyr1]-apelin-13 administration required continuous infusion through osmotic pump to achieve a comparable effect [47]. Here we found that the lipoPEG-PA13 formulation, administered only once weekly, was capable of attenuating cardiac hypertrophy and the resulting dysfunction for up to two weeks post injury. It should be noted that the four animal groups studied showed varying levels of absolute FS at baseline (Fig. 5D); thus, we utilized percent change from baseline to correct for these differences (Fig. 5A–C). Hence, although the absolute FS of the TAC + apelin group was above that of the TAC + nanocarriers group at several time points in Fig. 5D, comparatively, the percentage improvement in contractility was significantly greater in the nanocarrier group, as demonstrated in Fig. 5C. Histology of the mouse hearts treated with lipoPEG-PA13 nanocarriers confirmed the *in vivo* effect of [Pyr1]-apelin-13 nanocarriers in diminishing fibrosis and cardiac hypertrophy two weeks post injury (Fig. 5E).

The *in vivo* drug release study performed on the TAC, sham-operated, and wild type (with no surgery) mice revealed the significant effect of the lipoPEG nano-capsulation in prolonging the apelin-13 lifetime in the blood plasma for up to 6 days (Fig. 6). This is while regular commercial apelin appears rapidly clears from the blood circulation, with a drastically short plasma half-life (no longer than 8 min) [46]. Remarkably, the effect of nanocarriers in sustained [Pyr1]-apelin-13 release was more significant in the TAC mice, in comparison with that in sham controls. This can be related to the induced changes in plasma proteins due to the acute cardiac (TAC) injury and/or the stress caused by surgery (known as the acute phase response) [75–79]. It is well recognized that the surface of nanocarriers gets covered by various proteins upon their entrance into the biological fluid (e.g., blood [58,80]). The type, amount, and thickness of the associated proteins on the surface of nanocarriers (so called "*protein corona*") can define their biological fate [81]. Since the protein source determines the type and composition of associated proteins on the surface of these carriers [82], the variation of plasma proteins in TAC-operated mice may change the protein corona thickness and composition, hence, leading to a prolonged blood circulation time. Further assessment of the potential role of protein corona formation on the drug release from nanocarriers would be of interest for the future investigations.

5. Conclusions

In summary, we have developed an engineered nanocarrier system, consisting of liposomal nanocarriers incorporating PEG polymer, that demonstrated significantly enhanced efficacy compared to the non-encapsulated, commercially available [Pyr1]-apelin-13, in the delivery and sustained release of drug both *in vitro* and *in vivo*. Administration of [Pyr1]-apelin-13 nanocarriers significantly attenuated left ventricular hypertrophy and pressure overload-induced cardiac dysfunction in the mouse model of TAC. An increase in the particles polydispersity could be a further beneficial way to prolong the release. Testing release characteristics of a highly-polydisperse particle formulation would be of interest for the future studies. Further investigations on other therapeutic factors that can be delivered using these carriers, and modification and/or optimization of these devices can establish a new generation of drug delivery systems with unprecedented efficacy to treat various heart injuries and diseases.

Acknowledgments

This work was supported by National Institutes of Health grants HL65484 and HL086879 (to PRL) and NIH R01 HL095571 (to JCW). VS was an Oak Foundation postdoctoral fellow at Stanford. SM was supported by T32 HL094274. We thank Chris Wagstrom, BioADD, Stanford, for helping with mass spec experiments.

Abbreviations

LipoPEG-PA13	liposome-PEG-[Pyr1]-apelin-13
PEG	polyethylene glycol
TAC	transverse aortic constriction
LV	left ventricle
LVIDd	left ventricle internal diameter at end diastole
LVIDs	left ventricle internal diameter at end systole
LVPWd	left ventricle posterior wall thickness at end diastole
LVPWs	left ventricle posterior wall thickness at end systole
FS	fractional shortening
AFM	atomic force microscopy

HEK human embryonic kidney
APP acute phase protein

Appendix A. Supplementary data

Supplementary data related to this article can be found at http://dx.doi.org/10.1016/j.biomaterials.2014.08.045.

References

[1] Frey N, Katus HA, Olson EN, Hill JA. Hypertrophy of the heart: a new therapeutic target? Circulation 2004;109:1580–9.
[2] Frey N, Olson EN. Cardiac hypertrophy: the good, the bad, and the ugly. Annu Rev Physiol 2003;65:45–79.
[3] Yoshida H, Imataki K, Nagahana H, Ihoriya F, Nakao Y, Saito D, et al. Cardiac hypertrophy in hypertrophic cardiomyopathy and hypertension evaluated by echocardiography and body surface isopotential mapping. J Cardiogr 1986;16:399–406.
[4] Levy D, Garrison RJ, Savage DD, Kannel WB, Castelli WP. Prognostic implications of echocardiographically determined left ventricular mass in the Framingham heart study. N Engl J Med 1990;322:1561–6.
[5] Koren MJ, Devereux RB, Casale PN, Savage DD, Laragh JH. Relation of left ventricular mass and geometry to morbidity and mortality in uncomplicated essential hypertension. Ann Intern Med 1991;114:345–52.
[6] Olson EN. A decade of discoveries in cardiac biology. Nat Med 2004;10:467–74.
[7] Iemitsu M, Miyauchi T, Maeda S, Sakai S, Kobayashi T, Fujii N, et al. Physiological and pathological cardiac hypertrophy induce different molecular phenotypes in the rat. Am J Physiol Regul Integr Comp Physiol 2001;281:R2029–36.
[8] deAlmeida AC, van Oort RJ, Wehrens XHT. Transverse aortic constriction in mice. J Vis Exp JoVE 2010;38:1729–31.
[9] Van Nierop BJ, van Assen HC, van Deel ED, Niesen LBP, Duncker DJ, Strijkers GJ, et al. Phenotyping of left and right ventricular function in mouse models of compensated hypertrophy and heart failure with cardiac MRI. PLoS ONE 2013;8:e55424.
[10] Patten RD, Hall-Porter MR. Small animal models of heart failure development of novel therapies, past and present. Circ Heart Fail 2009;2:138–44.
[11] Rockman HA, Ross RS, Harris AN, Knowlton KU, Steinhelper ME, Field LJ, et al. Segregation of atrial-specific and inducible expression of an atrial natriuretic factor transgene in an in vivo murine model of cardiac hypertrophy. Proc Natl Acad Sci U S A 1991;88:8277–81.
[12] Liao Y, Ishikura F, Beppu S, Asakura M, Takashima S, Asanuma H, et al. Echocardiographic assessment of LV hypertrophy and function in aortic-banded mice: necropsy validation. Am J Physiol Heart Circ Physiol 2002;282:H1703–8.
[13] Nakamura A, Rokosh DG, Paccanaro M, Yee RR, Simpson PC, Grossman W, et al. LV systolic performance improves with development of hypertrophy after transverse aortic constriction in mice. Am J Physiol Heart Circ Physiol 2001;281:H1104–12.
[14] Koguchi W, Kobayashi N, Takeshima H, Ishikawa M, Sugiyama F, Ishimitsu T. Cardioprotective effect of apelin-13 on cardiac performance and remodeling in end-stage heart failure. Circ J Off J Jpn Circ Soc 2012;76:137–44.
[15] Zhang B-H, Guo C-X, Wang H-X, Lu L-Q, Wang Y-J, Zhang L-K, et al. Cardioprotective effects of adipokine apelin on myocardial infarction. Heart Vessels 2013.
[16] Simpkin JC, Yellon DM, Davidson SM, Lim SY, Wynne AM, Smith CCT. Apelin-13 and apelin-36 exhibit direct cardioprotective activity against ischemia-reperfusion injury. Basic Res Cardiol 2007;102:518–28.
[17] Lee DK, Cheng R, Nguyen T, Fan T, Kariyawasam AP, Liu Y, et al. Characterization of apelin, the ligand for the APJ receptor. J Neurochem 2000;74:34–41.
[18] Szokodi I, Tavi P, Földes G, Voutilainen-Myllylä S, Ilves M, Tokola H, et al. Apelin, the novel endogenous ligand of the orphan receptor APJ, regulates cardiac contractility. Circ Res 2002;91:434–40.
[19] El Messari S, Iturrioz X, Fassot C, De Mota N, Roesch D, Llorens-Cortes C. Functional dissociation of apelin receptor signaling and endocytosis: implications for the effects of apelin on arterial blood pressure. J Neurochem 2004;90:1290–301.
[20] Kuba K, Zhang L, Imai Y, Arab S, Chen M, Maekawa Y, et al. Impaired heart contractility in Apelin gene-deficient mice associated with aging and pressure overload. Circ Res 2007;101:e32–42.
[21] Ashley EA, Powers J, Chen M, Kundu R, Finsterbach T, Caffarelli A, et al. The endogenous peptide apelin potently improves cardiac contractility and reduces cardiac loading in vivo. Cardiovasc Res 2005;65:73–82.
[22] Maguire JJ, Kleinz MJ, Pitkin SL, Davenport AP. [Pyr1]apelin-13 identified as the predominant apelin isoform in the human heart: vasoactive mechanisms and inotropic action in disease. Hypertension 2009;54:598–604.
[23] Wang W, McKinnie SMK, Patel VB, Haddad G, Wang Z, Zhabyeyev P, et al. Loss of apelin exacerbates myocardial infarction adverse remodeling and ischemia-reperfusion injury: therapeutic potential of synthetic apelin analogues. J Am Heart Assoc 2013;2:e000249.
[24] Tatemoto K, Hosoya M, Habata Y, Fujii R, Kakegawa T, Zou MX, et al. Isolation and characterization of a novel endogenous peptide ligand for the human APJ receptor. Biochem Biophys Res Commun 1998;251:471–6.
[25] Murza A, Belleville K, Longpré J-M, Sarret P, Marsault E. Stability and degradation patterns of chemically modified analogs of apelin-13 in plasma and cerebrospinal fluid. Biopolymers 2014;101:293–303.
[26] Azizi Y, Faghihi M, Imani A, Roghani M, Nazari A. Post-infarct treatment with [Pyr1]-apelin-13 reduces myocardial damage through reduction of oxidative injury and nitric oxide enhancement in the rat model of myocardial infarction. Peptides 2013;46:76–82.
[27] Brito L, Amiji M. Nanoparticulate carriers for the treatment of coronary restenosis. Int J Nanomed 2007;2:143–61.
[28] Yuan A, Wu J, Song C, Tang X, Qiao Q, Zhao L, et al. A novel self-assembly albumin nanocarrier for reducing doxorubicin-mediated cardiotoxicity. J Pharm Sci 2013;102:1626–35.
[29] Donaldson K, Duffin R, Langrish JP, Miller MR, Mills NL, Poland CA, et al. Nanoparticles and the cardiovascular system: a critical review. Nanomed 2013;8:403–23.
[30] Gunaseelan S, Gunaseelan K, Deshmukh M, Zhang X, Sinko PJ. Surface modifications of nanocarriers for effective intracellular delivery of anti-HIV drugs. Adv Drug Deliv Rev 2010;62:518–31.
[31] Allen TM, Cullis PR. Liposomal drug delivery systems: from concept to clinical applications. Adv Drug Deliv Rev 2013;65:36–48.
[32] Medina OP, Zhu Y, Kairemo K. Targeted liposomal drug delivery in cancer. Curr Pharm Des 2004;10:2981–9.
[33] Fleisher D, Niemiec SM, Oh CK, Hu Z, Ramachandran C, Weiner N. Topical delivery of growth hormone releasing peptide using liposomal systems: an in vitro study using hairless mouse skin. Life Sci 1995;57:1293–7.
[34] Malam Y, Loizidou M, Seifalian AM. Liposomes and nanoparticles: nanosized vehicles for drug delivery in cancer. Trends Pharmacol Sci 2009;30:592–9.
[35] Kumar P, Gulbake A, Jain SK. Liposomes a vesicular nanocarrier: potential advancements in cancer chemotherapy. Crit Rev Ther Drug Carr Syst 2012;29:355–419.
[36] Lestini BJ, Sagnella SM, Xu Z, Shive MS, Richter NJ, Jayaseharan J, et al. Surface modification of liposomes for selective cell targeting in cardiovascular drug delivery. J Control Release Off J Control Release Soc 2002;78:235–47.
[37] Drummond DC, Meyer O, Hong K, Kirpotin DB, Papahadjopoulos D. Optimizing liposomes for delivery of chemotherapeutic agents to solid tumors. Pharmacol Rev 1999;51:691–744.
[38] Waterhouse DN, Madden TD, Cullis PR, Bally MB, Mayer LD, Webb MS. Preparation, characterization, and biological analysis of liposomal formulations of vincristine. Methods Enzymol 2005;391:40–57.
[39] Haran G, Cohen R, Bar LK, Barenholz Y. Transmembrane ammonium sulfate gradients in liposomes produce efficient and stable entrapment of amphipathic weak bases. Biochim Biophys Acta BBA – Biomembr 1993;1151:201–15.
[40] Xu H, Deng Y, Chen D, Hong W, Lu Y, Dong X. Esterase-catalyzed dePEGylation of pH-sensitive vesicles modified with cleavable PEG-lipid derivatives. J Control Release Off J Control Release Soc 2008;130:238–45.
[41] Chen Z, Deng, Zhao, Tao. Cyclic RGD peptide-modified liposomal drug delivery system: enhanced cellular uptake in vitro and improved pharmacokinetics in rats. Int J Nanomed 2012:3803.
[42] El Maghraby GMM, Williams AC, Barry BW. Drug interaction and location in liposomes: correlation with polar surface areas. Int J Pharm 2005;292:179–85.
[43] Tamargo J, Duarte J, Caballero R, Delpón E. New therapeutic targets for the development of positive inotropic agents. Discov Med 2011;12:381–92.
[44] Andersen CU, Hilberg O, Mellemkjaer S, Nielsen-Kudsk JE, Simonsen U. Apelin and pulmonary hypertension. Pulm Circ 2011;1:334–46.
[45] Mesmin C, Renvoisé M, Becher F, Ezan E, Fenaille F. MS-based approaches to unravel the molecular complexity of proprotein-derived biomarkers and support their quantification: the examples of B-type natriuretic peptide and apelin peptides. Bioanalysis 2012;4:2851–63.
[46] Japp AG, Cruden NL, Amer DAB, Li VKY, Goudie EB, Johnston NR, et al. Vascular effects of apelin in vivo in man. J Am Coll Cardiol 2008;52:908–13.
[47] Scimia MC, Hurtado C, Ray S, Metzler S, Wei K, Wang J, et al. APJ acts as a dual receptor in cardiac hypertrophy. Nature 2012;488:394–8.
[48] Parasuraman S, Raveendran R, Kesavan R. Blood sample collection in small laboratory animals. J Pharmacol Pharmacother 2010;1:87–93.
[49] Pitkin SL, Maguire JJ, Kuc RE, Davenport AP. Modulation of the apelin/APJ system in heart failure and atherosclerosis in man. Br J Pharmacol 2010;160:1785–95.
[50] Japp AG, Cruden NL, Barnes G, van Gemeren N, Mathews J, Adamson J, et al. Acute cardiovascular effects of apelin in humans potential role in patients with chronic heart failure. Circulation 2010;121:1818–27.
[51] Katugampola SD, Maguire JJ, Matthewson SR, Davenport AP. [(125)I]-(Pyr(1))Apelin-13 is a novel radioligand for localizing the APJ orphan receptor in human and rat tissues with evidence for a vasoconstrictor role in man. Br J Pharmacol 2001;132:1255–60.
[52] Tasci I, Dogru T, Naharci I, Erdem G, Yilmaz MI, Sonmez A, et al. Plasma apelin is lower in patients with elevated LDL-cholesterol. Exp Clin Endocrinol Diabetes Off J Ger Soc Endocrinol Ger Diabetes Assoc 2007;115:428–32.
[53] Leeper NJ, Tedesco MM, Kojima Y, Schultz GM, Kundu RK, Ashley EA, et al. Apelin prevents aortic aneurysm formation by inhibiting macrophage inflammation. Am J Physiol Heart Circ Physiol 2009;296:H1329–35.

[54] Kleinz MJ, Baxter GF. Apelin reduces myocardial reperfusion injury independently of PI3K/Akt and P70S6 kinase. Regul Pept 2008;146:271–7.
[55] Mahmoudi M, Sant S, Wang B, Laurent S, Sen T. Superparamagnetic iron oxide nanoparticles (SPIONs): development, surface modification and applications in chemotherapy. Adv Drug Deliv Rev 2011;63:24–46.
[56] Kumar A, Zhang X, Liang X-J. Gold nanoparticles: emerging paradigm for targeted drug delivery system. Biotechnol Adv 2013;31:593–606.
[57] De Jong WH, Borm PJ. Drug delivery and nanoparticles: applications and hazards. Int J Nanomed 2008;3:133–49.
[58] Mahmoudi M, Lynch I, Ejtehadi MR, Monopoli MP, Bombelli FB, Laurent S. Protein-nanoparticle interactions: opportunities and challenges. Chem Rev 2011;111:5610–37.
[59] Mahon E, Salvati A, Baldelli Bombelli F, Lynch I, Dawson KA. Designing the nanoparticle-biomolecule interface for "targeting and therapeutic delivery". J Control Release Off J Control Release Soc 2012;161:164–74.
[60] Jia ZQ, Hou L, Leger A, Wu I, Kudej AB, Stefano J, et al. Cardiovascular effects of a PEGylated apelin. Peptides 2012;38:181–8.
[61] Roberts MJ, Bentley MD, Harris JM. Chemistry for peptide and protein PEGylation. Adv Drug Deliv Rev 2002;54:459–76.
[62] Rezler EM, Khan DR, Tu R, Tirrell M, Fields GB. Peptide-mediated targeting of liposomes to tumor cells. Methods Mol Biol Clifton N. J 2007;386:269–98.
[63] Rezler EM, Khan DR, Lauer-Fields J, Cudic M, Baronas-Lowell D, Fields GB. Targeted drug delivery utilizing protein-like molecular architecture. J Am Chem Soc 2007;129:4961–72.
[64] Chono S, Fukuchi R, Seki T, Morimoto K. Aerosolized liposomes with dipalmitoyl phosphatidylcholine enhance pulmonary insulin delivery. J Control Release Off J Control Release Soc 2009;137:104–9.
[65] Harris JM, Chess RB. Effect of pegylation on pharmaceuticals. Nat Rev Drug Discov 2003;2:214–21.
[66] Lee H, Jang IH, Ryu SH, Park TG. N-terminal site-specific mono-pegylation of epidermal growth factor. Pharm Res 2003;20:818–25.
[67] Visser CC, Stevanović S, Voorwinden LH, van Bloois L, Gaillard PJ, Danhof M, et al. Targeting liposomes with protein drugs to the blood-brain barrier in vitro. Eur J Pharm Sci Off J Eur Fed Pharm Sci 2005;25:299–305.
[68] Xie Y, Ye L, Zhang X, Cui W, Lou J, Nagai T, et al. Transport of nerve growth factor encapsulated into liposomes across the blood-brain barrier: in vitro and in vivo studies. J Control Release Off J Control Release Soc 2005;105:106–19.
[69] Robinson SN, Talmadge JE. Sustained release of growth factors. Vivo Athens Greece 2002;16:535–40.
[70] Woodle MC, Matthay KK, Newman MS, Hidayat JE, Collins LR, Redemann C, et al. Versatility in lipid compositions showing prolonged circulation with sterically stabilized liposomes. Biochim Biophys Acta 1992;1105:193–200.
[71] Kim A, Yun MO, Oh YK, Ahn WS, Kim CK. Pharmacodynamics of insulin in polyethylene glycol-coated liposomes. Int J Pharm 1999;180:75–81.
[72] Choi KY, Yoon HY, Kim J-H, Bae SM, Park R-W, Kang YM, et al. Smart nanocarrier based on PEGylated hyaluronic acid for cancer therapy. ACS Nano 2011;5:8591–9.
[73] Fenske DB, Palmer LR, Chen T, Wong KF, Cullis PR. Cationic poly(-ethyleneglycol) lipids incorporated into pre-formed vesicles enhance binding and uptake to BHK cells. Biochim Biophys Acta 2001;1512:259–72.
[74] Kibria G, Hatakeyama H, Ohga N, Hida K, Harashima H. Dual-ligand modification of PEGylated liposomes shows better cell selectivity and efficient gene delivery. J Control Release Off J Control Release Soc 2011;153:141–8.
[75] Rosenson S. R. Myocardial injury: the acute phase response and lipoprotein metabolism. J Am Coll Cardiol 1993;22:933–40.
[76] Mackiewicz A, Kushner I, Baumann H. Acute phase proteins molecular biology, biochemistry, and clinical applications. CRC Press; 1993.
[77] Gruys E, Toussaint MJM, Niewold TA, Koopmans SJ. Acute phase reaction and acute phase proteins. J Zhejiang Univ Sci B 2005;6:1045–56.
[78] Sanchez O, Arnau A, Pareja M, Poch E, Ramirez I, Soley M. Acute stress-induced tissue injury in mice: differences between emotional and social stress. Cell Stress Chaperones 2002;7:36–46.
[79] Cray C, Zaias J, Altman NH. Acute phase response in animals: a review. Comp Med 2009;59:517–26.
[80] Monopoli MP, Åberg C, Salvati A, Dawson KA. Biomolecular coronas provide the biological identity of nanosized materials. Nat Nanotechnol 2012;7:779–86.
[81] Monopoli MP, Walczyk D, Campbell A, Elia G, Lynch I, Baldelli Bombelli F, et al. Physical–chemical aspects of protein corona: relevance to in vitro and in vivo biological impacts of nanoparticles. J Am Chem Soc 2011;133:2525–34.
[82] Hajipour MJ, Laurent S, Aghaie A, Rezaee F, Mahmoudi M. Personalized protein coronas: a "key" factor at the nanobiointerface. Biomater Sci 2014;2:1210–21.